Next-generation mobile communication leveraging cutting-edge photonic technologies (Photonic 6G)

Photonic THz detection based on carrier conversion from terahertz wave to dual-wavelength near-infrared light injection-locked to optical frequency comb via electro-optic polymer modulator.

Yudai Matsumura[1], Yu Tokizane[1], Eiji Hase[1], Naoya Kuse[1], Takeo Minamikawa[1,2], Junichi Fujikata[1], Hiroki Kishikawa[1], Masanobu Haraguchi[1], Yasuhiro Okamura[1,3], Takahiro Kaji[4], Akira Otomo[4], Isao Morohashi[4], Atsushi Kanno[4,5], Shintaro Hisatake[6] and Takeshi Yasui[1]

[1] Institute of Post-LED Photonics (pLED), Tokushima University, 2-1, Minami-Josanjima, Tokushima 770-8506, Japan

[2] Graduate School of Engineering Science, Osaka University, 1-3 Machikaneyama, Toyonaka, Osaka 560-8531, Japan

[3] Center for Higher Education and Digital Transformation, University of Yamanashi, 4-4-37 Takeda, Kofu, Yamanashi 400-8510, Japan

[4] National Institute of Information and Communications Technology, 588-2 Iwaoka, Nishi-ku, Kobe, Hyogo, 651-2492, and 4-2-1 Nukuikitamachi, Koganei, Tokyo 184-8795, Japan

[5] Department of Electrical and Mechanical Engineering, Nagoya Institute of Technology, Gokiso-cho, Showa-ku, Nagoya, Aichi 466-8555, Japan

[6] Electrical and Energy System Engineering Division, Gifu University, 1-1 Yanagido, Gifu 501-1193, Japan

The development of wireless communication technologies has witnessed tremendous advancements over recent decades, culminating in the widespread deployment of 5G networks. However, as we look forward to the next generation, 6G, there are significant technical challenges to overcome. One of the key issues is the use of extremely high frequencies, exceeding 300 GHz, which introduces limitations such as increasing phase noise and power consumption in traditional electronic devices and systems. This necessitates a shift towards photonic technologies, which offer superior performance in these frequency ranges (Nagatsuma, Ducournau and Renaud, 2016).

Terahertz (THz) waves, positioned within this high-frequency spectrum, present a promising solution for 6G wireless communication (Dang *et al.*, 2020). To achieve such 6G wireless communication, a crucial technology is, of course, THz generation and THz detection. The photonic generation of THz waves, particularly using optical frequency combs (OFCs) (Udem, Holzwarth and Hänsch, 2002) together with the help of a uni-travelling carrier photodiode (UTC-PD) for photomixing (Ishibashi and Ito, 2020), has shown great potential due to their low phase noise and precise frequency control (Figure 1, top left). For example, soliton microcombs (Shen *et al.*, 2020), generated within on-chip Kerr microresonators, have garnered significant interest for their ability to produce ultralow-phase-noise THz waves at frequencies like 300 GHz (Zhang *et al.*, 2019; Tetsumoto *et al.*, 2021) and 560 GHz (Kuse *et al.*, 2022). This interest stems from the fact that the frequency spacing (f_{rep}) of these soliton microcombs is naturally close to the desired THz frequency (f_{THz}). Consequently, adjacent modes within the microcomb can be utilised directly for photomixing, leveraging the inherent low-phase-noise characteristics of f_{rep} while avoiding complications associated with optical frequency multiplication.

Regarding the detection of THz waves, electronic THz detectors, such as Schottky barrier diodes and mixers, have still been used in THz wireless communication regardless of bulky, fragile, complicated and expensive characteristics. The situation of THz detection might be improved with the introduction of photonic technology in the same manner as THz generation. For example, the realisation of carrier conversion from THz waves to near-infrared (NIR) light through photonic technology holds the potential to leverage existing optical communication infrastructure with minimal adjustments (Figure 1, top right). This approach would facilitate the photonic detection of THz signals, thereby enabling a seamless integration between wireless and optical communication networks. A promising technique for achieving THz-to-NIR carrier conversion is non-polarimetric electro-optic (EO) down-conversion (NP-EO-DC), which has previously been employed in the visualisation of millimetre-wave electric fields (Hisatake, Pham and Nagatsuma, 2014). In this approach, dual-wavelength NIR light serves as the optical carrier, with modulation sidebands induced by millimetre-wave frequencies being generated through the EO effect. When the frequency spacing of the dual-wavelength NIR light aligns closely with that of the millimetre-wave signal, an optical beat signal emerges within the RF spectrum between one of the NIR beams and the corresponding modulation sideband. The heterodyne detection of this optical beat signal amplifies the RF beat signal, effectively producing the desired baseband signal. In this NP-EO-DC, the generation of dual-wavelength NIR light with a constant optical frequency spacing and phase synchronisation is crucial, and OFCs can play a significant role in this generation. In other words, OFCs are essential not only for photonic THz generation but also for photonic THz detection.

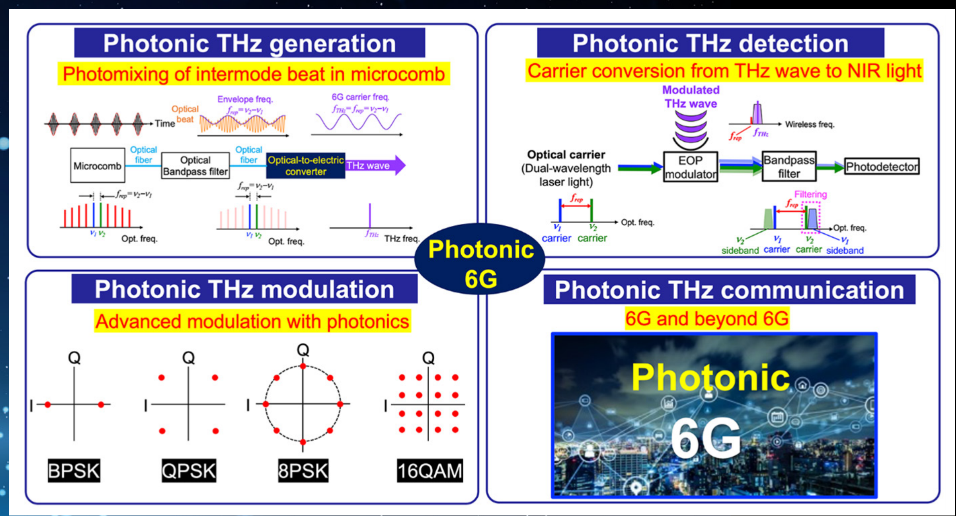

Figure 1: 6G boosted by advanced photonics (Photonic 6G).

In this study, we explore the feasibility of this approach by demonstrating THz-to-NIR carrier conversion, utilising high signal-to-noise ratio (SNR) dual-wavelength NIR light generated through optical injection locking of NIR distributed feedback laser diode (DFB) to an OFC (Matsumura *et al.*, 2023a, 2023b). An electro-optic polymer (EOP) modulator is used for a highly efficient THz-to-NIR carrier converter (Kaji *et al.*, 2021; 2023). The demonstrated proof-of-concept experiment serves as a crucial step towards integrating photonic detection into the broader framework of 6G wireless communication.

Principle of operation

Optical injection locking (OIL)

The principle of OIL involves synchronising a slave laser with a master laser by injecting light from the master laser into the slave laser. This synchronisation occurs when the injected light forces the slave laser to lock its frequency, phase, and even output power to the characteristics of the master laser. Here, we consider one optical frequency mode extracted from OFC (OFC mode) for a master laser and DFB for a slave laser (see Figure 2). Initially, the DFB operates at its natural frequency. However, upon injection of the OFC mode, the DFB's frequency is pulled toward the frequency of the injected OFC mode. When the injection strength is sufficient, the DFB locks to the OFC mode's frequency, operating at this locked frequency (namely, OIL-DFB). Besides frequency, the phase of the OIL-DFB also locks to the phase of the injected OFC mode. Injection locking reduces the linewidth of the DFB, enhancing its spectral purity. This is particularly beneficial when using the DFB, which typically has a broader linewidth compared to the narrow lines of the OFC mode. This process effectively forces the DFB to oscillate at the frequency and phase determined by the OFC mode. By using a highly stable OFC mode and a high-power DFB in OIL, it is possible to obtain a laser light that combines the characteristics of both high stability and high power.

Next, consider the case where two DFBs operating at different wavelengths are respectively optical-injection-locked to two different modes of the OFC. Since the frequency spacing of the OFC is strictly constant and all OFC modes are phase-locked, a pair of OIL-DFBs will have a constant optical frequency spacing and synchronised optical phase. The constant frequency spacing and phase synchronisation are crucial characteristics for the two-wavelength NIR carrier used in THz-to-NIR carrier conversion.

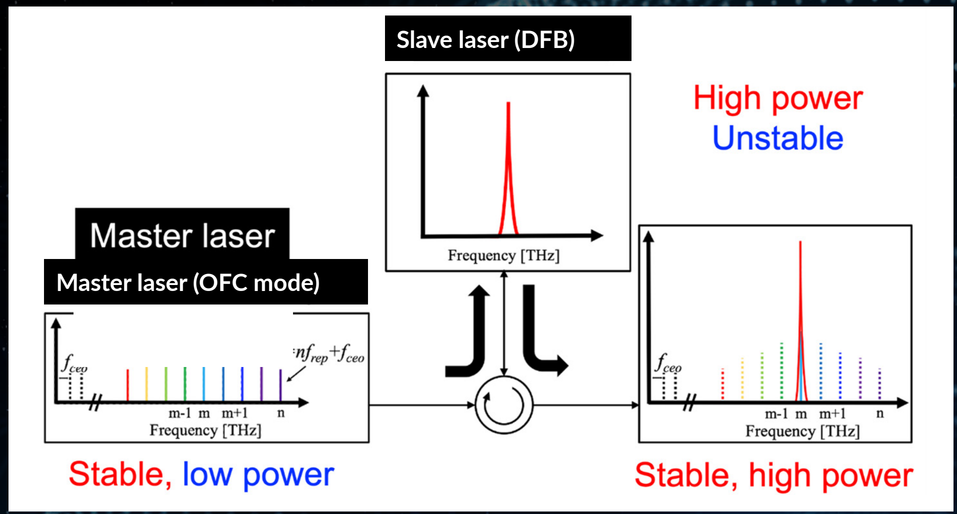

Figure 2: Principle of optical injection locking.

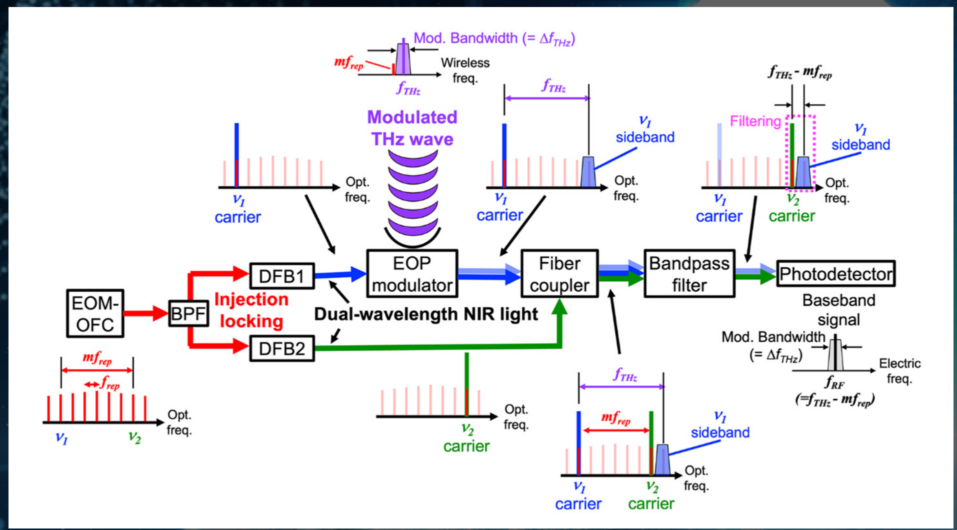

Figure 3: Principle of THz-to-NIR carrier conversion.

THz-to-NIR carrier conversion

The core mechanism of the carrier conversion process from a modulated THz wave to dual-wavelength NIR light is illustrated in Figure 3. The system operates by employing a pair of high-power DFB, denoted as DFB1 and DFB2, whose optical frequencies (v_1 = 193.39 THz and v_2 = 193.49 THz, respectively; their optical frequency spacing = $v_2 - v_1$ ≈ 100 GHz) are spaced to closely match the frequency of the THz carrier (f_{THz} = 101 GHz, power = 4 dBm = 2.5 mW). The electro-optic-modulator OFC (EOM-OFC, centre wavelength = 1550 nm, f_{rep} = 10 GHz) generates two modes with a frequency spacing (mf_{rep} = $10f_{rep}$ = 100 GHz ≈ $v_2 - v_1$) that approximates f_{THz}. These modes are isolated via an optical bandpass filter (BPF) and respectively injected into DFBs, achieving OIL. This process corresponds to amplifying the selected OFC modes while suppressing unwanted EOM-OFC modes and reducing amplified spontaneous emission (ASE) background, resulting in a stable, high-power, dual-wavelength NIR output.

The modulated THz wave is introduced into the EOP modulator, where it interacts with the v_1 carrier propagating through the optical waveguide of the EOP modulator. This interaction induces phase modulation, producing modulation sidebands at frequencies separated by f_{THz} from v_1. Meanwhile, the v_2 carrier bypasses the EOP modulator and remains unmodulated. Due to the OIL, v_1 and v_2 maintain a phase-locked relationship, ensuring consistent frequency spacing.

An optical beat signal emerges between the v_2 carrier and the v_1 sideband, which is detected as a baseband signal by a photodetector after filtering out the v_1 carrier. The heterodyne detection method amplifies the weak v_1 sideband through its interaction with the strong v_2 carrier, resulting in a baseband signal corresponding to the modulated THz wave with a frequency of $f_{RF} = f_{THz} - mf_{rep}$ (= 1 GHz).

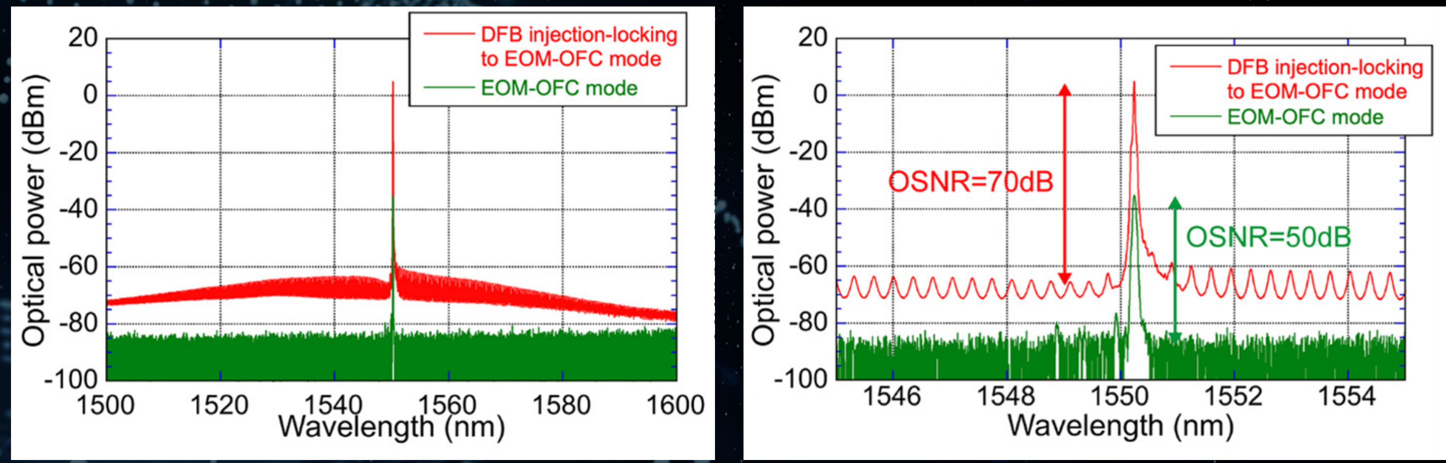

Figure 4: (a) Optical spectra of the DFB injection-locked to EOM-OFC mode (red plot) and extracted EOM-OFC mode (green plot) and (b) their magnified spectra. The resolution bandwidth of the optical spectrum is 0.02 nm.

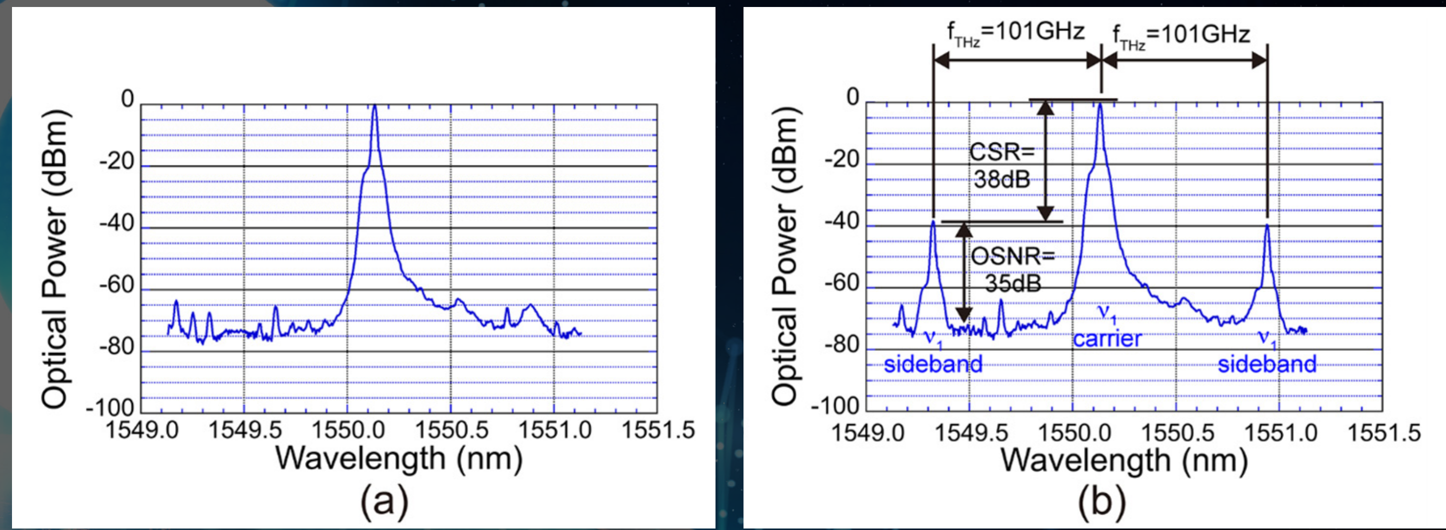

Figure 5: Optical spectra of (a) the v_1 carrier without irradiation of THz wave and (b) the v_1 carrier and its modulation sideband with irradiation of THz wave. The resolution bandwidth of the optical spectrum is 0.02 nm.

Experimental results

Optical injection locking of DFB to EOM-OFC mode

The performance of the OIL of the DFB to the EOM-OFC mode was first assessed. Figure 4(a) presents the optical spectrum of the DFB, with an optical power of 8 mW, optical-injection-locked to the EOM-OFC mode (OIL-DFB, see red plot). For comparison, the optical spectrum of the extracted EOM-OFC mode (optical power = 2 µW) is also shown (see green plot). The background noise of the EOM-OFC mode represents the noise floor of the optical spectrum analyser (resolution bandwidth or RBW = 0.02 nm). In contrast, the background noise of the OIL-DFB appears at a higher level due to weak luminescence from the DFB. Figure 4(b) shows the magnified optical spectrum, confirming that the OIL-DFB wavelength is identical to that of the extracted EOM-OFC mode, indicating successful OIL. While no difference in the linewidth of the DFB laser was observed before and after OIL, this is attributed to the insufficient RBW of the optical spectrum analyser. However, the reduction in linewidth due to OIL can be verified in the RF spectrum of the optical beat signal (not shown). Despite the presence of ultra-fine spectrally modulated luminescence associated with the internal grating structure of the DFB, its intensity remains significantly lower than that of the OIL-DFB, achieving an optical signal-to-noise ratio (OSNR) of 70 dB. Conversely, the OSNR of the extracted EOM-OFC mode remains approximately 50 dB, limited by the optical power and background noise. Thus, sufficient OSNR was obtained in the OIL-DFB for the generation of modulation sidebands using the EOP modulator.

Observation of THz-induced optical modulation sideband and its RF beat signal

The modulation sideband of the v_1 carrier was observed by irradiating the EOP

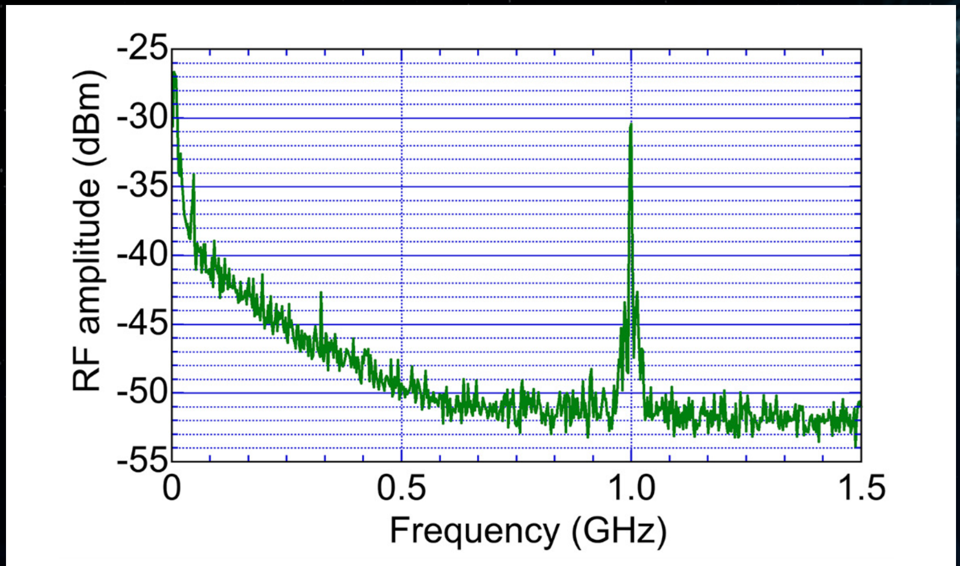

Figure 6: RF spectra of optical beat signal between the v_1 modulation sideband and the v_2 carrier. The resolution bandwidth and video bandwidth of the RF spectrum are 1MHz.

modulator with THz waves. Figures 5(a) and 5(b) compare the optical spectra at the output of the optical waveguide of the EOP modulator without and with THz wave irradiation (RBW = 0.02 nm). Only the v_1 carrier is present without THz irradiation, whereas both the v_1 carrier and its modulation sidebands are observed. Under THz irradiation, the modulation sidebands appear exactly $\pm f_{THz}$ (= 101 GHz) away from the v_1 carrier. The carrier-to-sideband ratio (CSR), defined as the ratio of the optical carrier to its modulation sideband, is 38 dB for the v_1 carrier and sideband pair. This improved CSR results from optimising the THz focus to match the shape of the patch antenna. The OSNR of the v_1 modulation sideband reaches 35 dB, thanks to the enhanced OSNR of the v_1 carrier via OIL. Based on the OSNR of the v_1 modulation sideband and the irradiated THz power (= 4 dBm = 2.5 mW), the minimum detectable THz power is estimated to be -29 dBm or 1.3 µW. Similar CSR and OSNR values should be maintained for the v_2 carrier and v_1 modulation sideband pair, which are close to each other.

Subsequently, the RF spectrum of the optical beat signal between the v_2 carrier and v_1 modulation sideband was measured. Figure 6 shows the RF spectrum of the beat signal (resolution bandwidth or RBW = video bandwidth or VBW = 1 MHz). Given that the frequency difference between f_{THz} (= 101 GHz) and $10f_{rep}$ (= 100 GHz) is 1 GHz, the RF beat signal appeared at 1 GHz with a SNR of 20 dB. The pronounced elevation in the spectrum at frequencies below 0.5 GHz is attributed to the noise signal from the amplifier following the photodetector. The SNR of the RF signal is expected to exhibit a linear dependence on the input THz power, as the detection of the 1 GHz RF signal relies on the optical heterodyning process between the v_1 modulation sideband and the v_2 carrier. While nonlinearity in the electro-optic Pockels effect in the EOP modulator could potentially influence the behaviour, it is anticipated to be negligible at the current THz power levels.

Photonic THz detection of 270-MHz on-off-keying THz signal

It is more practically significant when using modulated THz signals (e.g. on-off-keying or OOK) rather than the unmodulated THz signal of Figures 5 and 6. Here, we conducted preliminary experiments on carrier conversion from modulated THz waves to single-wavelength NIR light prior to the carrier conversion from modulated THz waves to two-wavelength NIR light. A modulated THz wave (carrier frequency = f_{THz} = 101 GHz, modulation frequency = Δf_{THz} = 270 MH) was generated from a frequency multiplier and irradiated onto an EOP modulator. Only the v_1 modulation sideband induced by the irradiated OOK-THz wave was optically extracted, and its baseband signal was measured by envelope detection. Figure 7 shows eye diagrams of (a) the transmitted OOK signal and (b) the received OOK-THz baseband signal. The eye diagram of the received OOK-THz baseband signal is clearly open, and the corresponding Q factor was 6.53. Future work will extend to carrier conversion from modulated THz waves to two-wavelength NIR light, which should enable support for higher bit-rate modulated THz waves through improved measurement SNR by optical heterodyned detection.

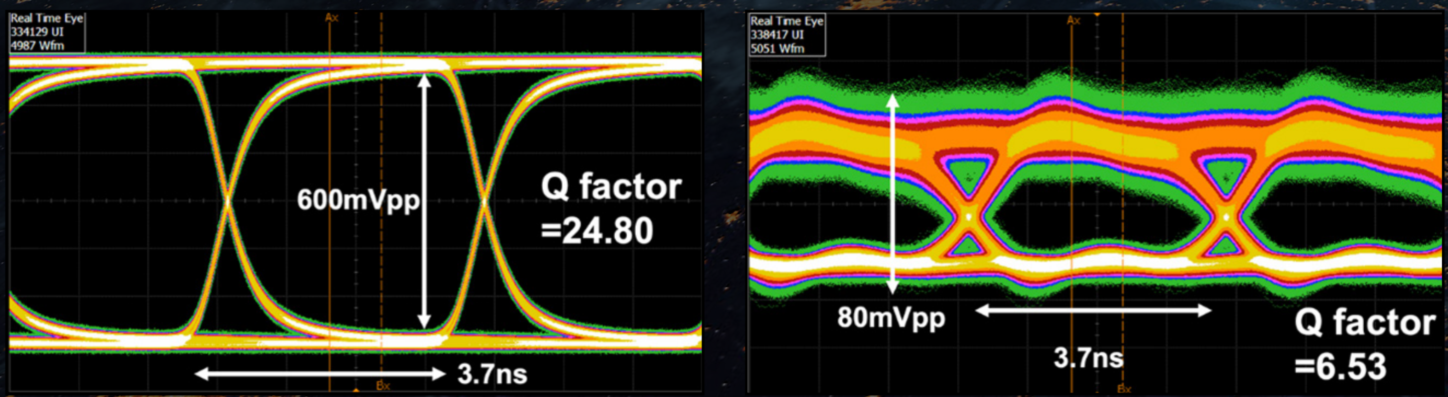

Figure 7: Eye diagrams of (a) the transmitted OOK signal (Q factor = 24.80) and (b) the received OOK-THz baseband signal (Q factor = 6.53).

Summary

This article has demonstrated the feasibility of THz-to-NIR carrier conversion using a combination of optical heterodyne-enhanced detection and high OSNR dual-wavelength DFBs optical-injection-locked to EOM-OFC mode, alongside a high-sensitivity EOP modulator. The resulting RF beat signal, corresponding to the unmodulated THz wireless carrier, achieved a SNR of 20 dB and exhibited excellent frequency stability. Furthermore, preliminary experiments demonstrated successful carrier conversion from modulated THz waves to single-wavelength NIR light, with a clear eye pattern and a Q factor of 6.53 for the received OOK-THz baseband signal. Future work aims to extend this approach to two-wavelength NIR light to support higher bit-rate modulated THz waves and improve measurement SNR.

The method proposed in this article represents a powerful tool for photonic THz detection in THz wireless communication systems, offering significant advantages in terms of SNR and frequency stability.

This study was supported by Ministry of Internal Affairs and Communications (JPJ000254), Cabinet Office, Government of Japan (Promotion of Regional Industries and Universities), Tokushima Prefecture, Japan (Creation and Application of Next-Generation Photonics) and Research Clusters programme of Tokushima University (2201001).

References

Dang, S., Amin, O., Shihada, B. and Alouini, M.-S. (2020) 'What should 6G be?', *Nature Electronics*, 3(1), pp. 20–29. doi: 10.1038/s41928-019-0355-6.

Hisatake, S., Pham, H.H.N. and Nagatsuma, T. (2014) 'Visualization of the spatial–temporal evolution of continuous electromagnetic waves in the terahertz range based on photonics technology', *Optica*, 1(6), pp. 365–371. doi: 10.1364/OPTICA.1.000365.

Ishibashi, T. and Ito, H. (2020) 'Uni-traveling-carrier photodiodes', *Journal of Applied Physics*, 127(3), 031101. doi: 10.1063/1.5129691.

Kaji, T., Morohashi, I., Tominari, Y., Sekine, N., Yamada, T. and Otomo, A. (2021) 'W-band optical modulators using electro-optic polymer waveguides and patch antenna arrays', *Optics Express*, 29(19), pp. 29604–29614. doi: 10.1364/OE.436678.

Kaji, T., Morohashi, I., Tominari, Y., Ohara, M., Yamada, T. and Otomo, A. (2023) 'D-band optical modulators using electro-optic polymer waveguides and non-coplanar patch antennas', *Optics Express*, 31(10), pp. 17112–17121. doi: 10.1364/OE.486457.

Kuse, N., Nishimoto, K., Tokizane, Y., Okada, S., Navickaite, G., Geiselmann, M., Minoshima, K. and Yasui, T. (2022) 'Low phase noise THz generation from a fiber-referenced Kerr microresonator soliton comb', *Communications Physics*, 5(1), 312. doi: 10.1038/s42005-022-00984-6.

Matsumura, Y., Tokizane, Y., Hase, E., Kuse, N., Minamikawa, T., Fujikata, J., Kishikawa, H., Haraguchi, M., Okamura, Y., Kaji, T., Otomo, A., Morohashi, I., Kanno, A., Hisatake, S. and Yasui, T. (2023a) 'Carrier conversion from terahertz wave to dual-wavelength near-infrared light for photonic terahertz detection in wireless communication', *Optics Express*, 31(20), pp. 33103–33112. doi: 10.1364/OE.480347.

Matsumura, Y., Hase, E., Tokizane, Y., Kuse, N., Fujikata, J., Kishikawa, H., Haraguchi, M., Okamura, Y., Kaji, T., Otomo, A., Kanno, A., Hisatake, S., and Yasui, T. (2023b) *Dual-λ, low-phase-noise, optical carrier for THz-to-optical carrier conversion with EOP modulator*. Available at: https://youtu.be/UMjlJpUlgNk.

Nagatsuma, T., Ducournau, G. and Renaud, C.C. (2016) 'Advances in terahertz communications accelerated by photonics', *Nature Photonics*, 10(6), pp. 371–379. doi: 10.1038/nphoton.2016.65.

Shen, B., Chang, L., Liu, J., Wang, H., Yang, Q.-F., Xiang, C., Wang, R.N., He, J., Liu, T., Xie, W., Guo, J., Kinghorn, D., Wu, L., Ji, Q.-X., Kippenberg, T.J., Vahala, K. and Bowers, J.E. (2020) 'Integrated turnkey soliton microcombs', *Nature*, 582(7810), pp. 365–369. doi: 10.1038/s41586-020-2421-5.

Tetsumoto, T., Nagatsuma, T., Fermann, M.E., Navickaite, G., Geiselmann, M. and Rolland, A. (2021) 'Optically referenced 300 GHz millimetre-wave oscillator', *Nature Photonics*, 15(7), pp. 516–522. doi: 10.1038/s41566-021-00801-w.

Udem, T., Holzwarth, R. and Hänsch, T.W. (2002) 'Optical frequency metrology', *Nature*, 416(6877), pp. 233–237. doi: 10.1038/416233a.

Zhang, S., Silver, J.M., Shang, X., Bino, L.D., Ridler, N.M. and Del'Haye, P. (2019) 'Terahertz wave generation using a soliton microcomb', *Optics Express*, 27(24), p. 35257. doi: 10.1364/OE.27.035257.

PROJECT NAME

PHOTONIC 6G

PROJECT SUMMARY

Our aim is to develop 'Photonic 6G', an all-photonic THz communication technology, by integrating advanced photonic methods. This includes generating low-phase-noise THz waves with microcombs and converting modulated THz waves into optical carrier signals. By leveraging these advancements, we aim to enable advanced modulation and multiplexing in the optical domain, ultimately achieving the integration for photonic 6G.

PROJECT PARTNERS

National Institute of Information and Communications Technology, Gifu University and Nagoya Institute of Technology.

PROJECT LEAD PROFILE

Professor Takeshi Yasui, based at Tokushima University, Japan, boasts a distinguished career in THz photonics. His work has led to THz comb, spectroscopy and imaging breakthroughs. He is the chief research officer in charge of the Institute of Post-LED Photonics. Prof. Yasui's research interests encompass THz photonics, optical comb and nonlinear microscopy, contributing significantly to advancements in these fields.

PROJECT CONTACTS

Professor Takeshi Yasui
Institute of Post-LED Photonics,
Tokushima University,
2-1, Minami-Josanjima,
Tokushima 770-8506, Japan
+81-88-656-7377
yasui.takeshi@tokushima-u.ac.jp
https://femto.me.tokushima-u.ac.jp/eng/
www.pled.tokushima-u.ac.jp/english/
https://www.youtube.com/channel/UCUkkVRVGtwdltwWs53U9m-A

FUNDING

This study was conducted as part of the contract "R&D of high-speed THz communication based on radio and optical direct conversion" (JPJ000254), which was established with the Ministry of Internal Affairs and Communications of Japan, the Cabinet Office of the Government of Japan (Promotion of Regional Industries and Universities), Tokushima Prefecture, Japan (Creation and Application of Next-Generation Photonics), and the Research Clusters programme of Tokushima University (2201001).